BEILSTEIN JOURNAL OF NANOTECHNOLOGY

Supporting Information

for

Fluorescent bioinspired albumin/polydopamine nanoparticles and their interactions with *Escherichia coli* cells

Eloïse Equy, Jordana Hirtzel, Sophie Hellé, Béatrice Heurtault, Eric Mathieu, Morgane Rabineau, Vincent Ball and Lydie Ploux

Beilstein J. Nanotechnol. **2023,** *14,* 1208–1224. doi:10.3762/bjnano.14.100

Additional tables and figures

Table S1: Mean hydrodynamic diameter and polydispersity index (PDI) of BSA/PDA NPs in Tris buffer 50 mM (without dialysis and freeze-drying).

	Ratio BSA/DA	Mean diameter in intensity (nm)	Mean diameter in number (nm)	PDI
BSA/PDA-NPs	0.25	83 ± 22	66 ± 16	0.21 ± 0.01
	1	32 ± 7	26 ± 6	0.32 ± 0.06
	3	18 ± 5	14 ± 3	0.27 ± 0.04
	6	15 ± 4	11 ± 3	0.27 ± 0.04
	10	15 ± 7	9 ± 3	0.27 ± 0.04
Ox-BSA/PDA-NPs	10	15 ± 4	11 ± 3	ND
RhBITC-BSA/PDA-NPs	10	28 ± 6	24 ± 3	0.57 ± 0.06
FITC BSA/PDA-NPs	10	17 ± 5	12 ± 3	0.19 ± 0.01

Table S2: Concentration, number of NPs per mL, and reaction yield of the as-prepared pristine BSA/PDA NPs solutions.

Ratio BSA/DA	Concentration (mg/mL)	Number of NPs /mL	Reaction Yield (%)
0.25	2	5×10^{15}	85
1	2	8×10^{16}	50
3	3	2×10^{14}	85
6	9	3×10^{18}	63
10	19	4×10^{15}	85

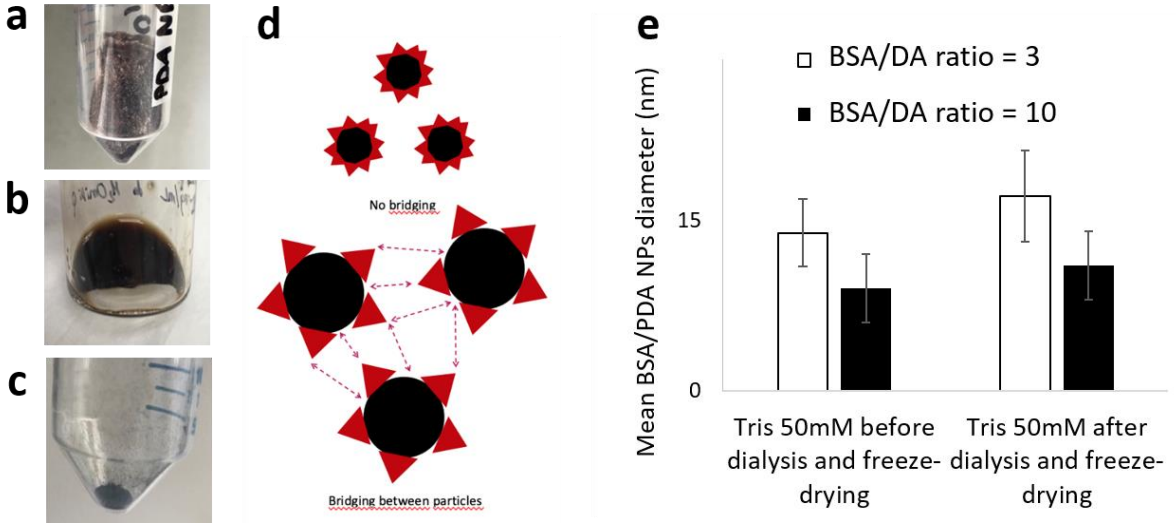

Figure S1: BSA/PDA NPs after freeze-drying. Pictures of (a) a foam obtained after freeze-drying of a BSA/PDA NPs suspension synthesized with a BSA/DA ratio of 3. (b) PDA/BSA NPs re-dissolved foam into Milli-Q® water (10mg/mL). (c) PDA/BSA-NPs ratio of 0.25 dehydrated powder. (d) Schematic of bridging between PDA/BSA-NPs. (e) PDA/BSA-NPs size variation due to dialysis and freeze-drying.

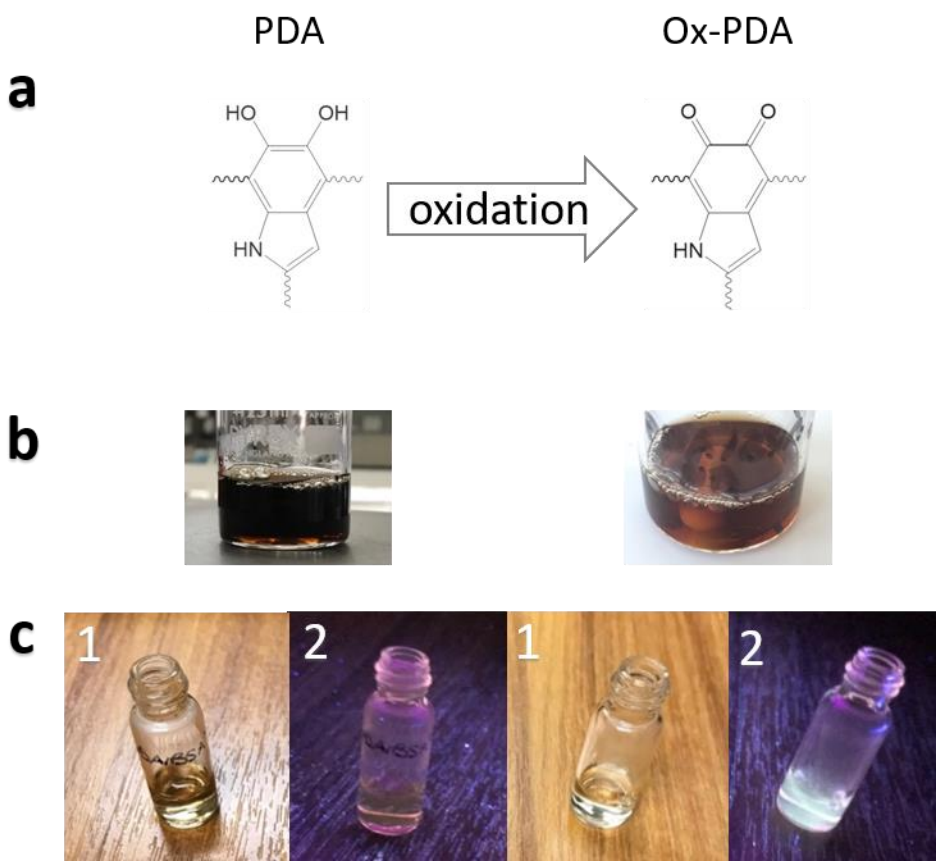

Figure S2: Oxidation of pristine BSA/PDA NPs providing fluorescent Ox-BSA/PDA NPs. (a) Reaction scheme of PDA (inspired from Ma et al. [1]). (b) Pictures of PDA/BSA-NPs suspensions after 1 h (left) or 24 h (right) of reaction with H_2O. (c) Pictures of PDA/BSA-NPs suspensions before (left) and after (right) oxidation (1) under natural light and (2) under UV light (365 nm).

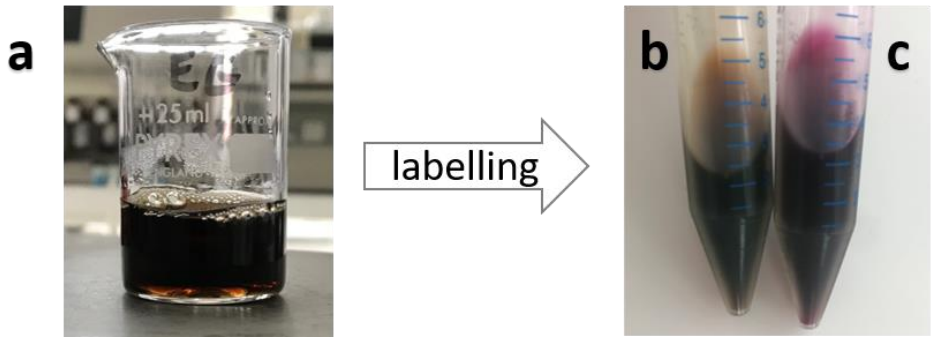

Figure S3: Pictures of FITC- and RhBITC-BSA/PDA NPs suspensions after dialysis with a 8–10 kDa cut-off membrane. (a) FITC-BSA/PDA NPs. (b) RhBITC-BSA/PDA NPs (c).

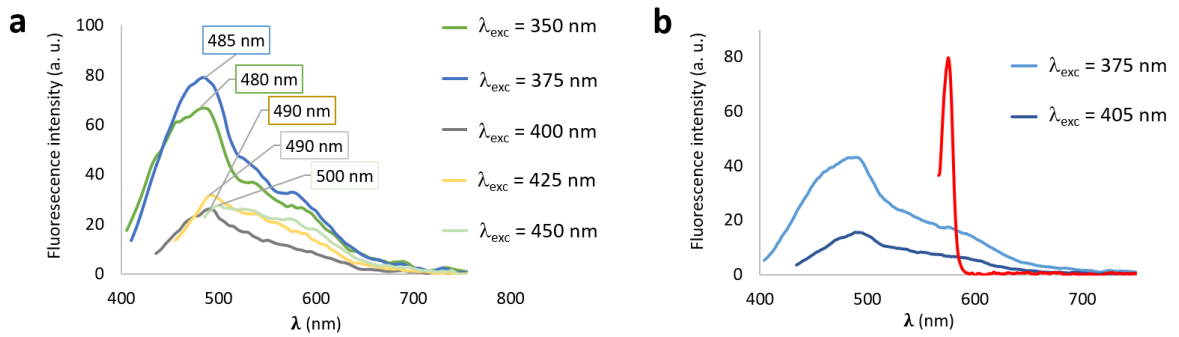

Figure S4: Absorption and emission spectra of Ox-PDA/BSA-NPs. (a) Emission spectra according to various excitation wavelengths (λ_{exc}) (PMT voltage at 1000 V); wavelengths corresponding to fluorescence intensity maxima are indicated in labels; spectra were smoothed by moving average method on 3 points. (b) Emission spectra of a mixture of Ox-PDA/BSA-NPs (3 mg/mL) and RhBITC (0.06 mg/mL) (95/5) under different excitation wavelengths (λ_{exc}) (PMT voltage at 900 V); spectra were smoothed by centered moving average method on 9, 9 and 3 points, respectively.

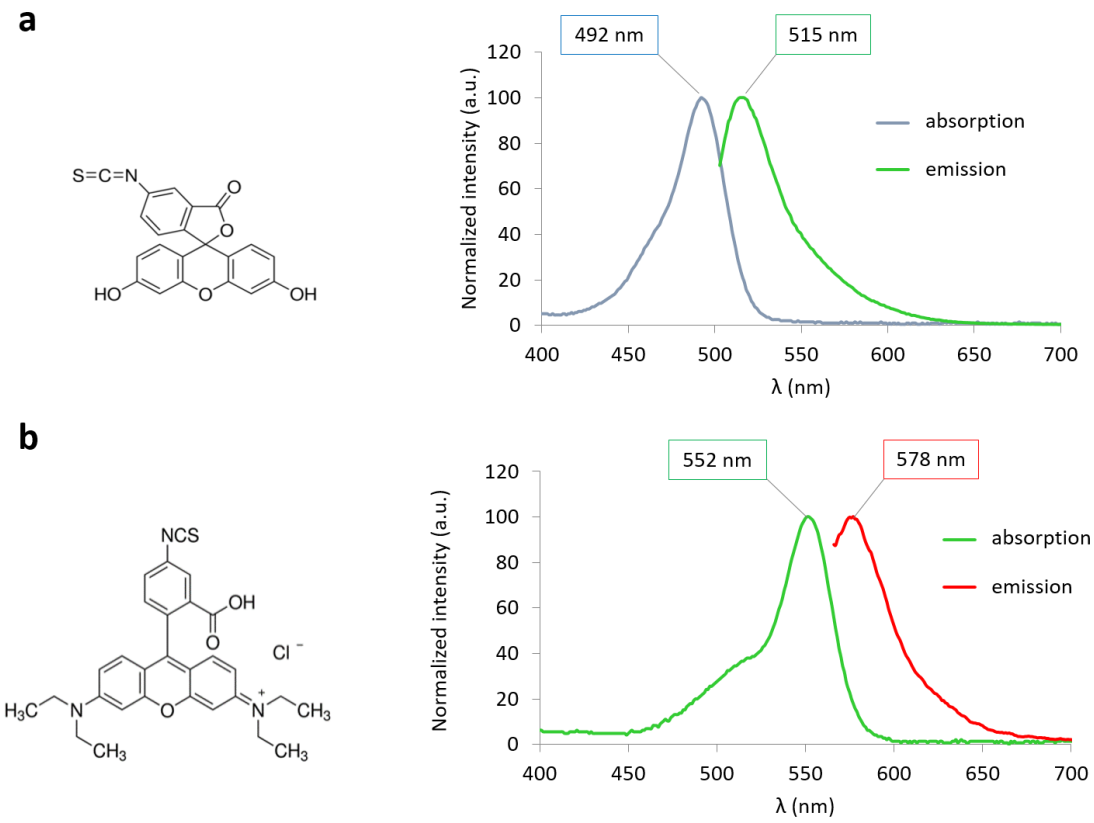

Figure S5: Absorption and emission spectra of free FITC and RhBITC. (a) Structure and normalized absorption and emission spectra of free FITC (164 µM) under excitation wavelength λ_{exc} of 488 nm. (b) Structure and normalized absorption and emission spectra of free RhBITC (373 µM) under excitation wavelength λ_{exc} of 550 nm. Spectra were smoothed by centered moving average method on 3 points.

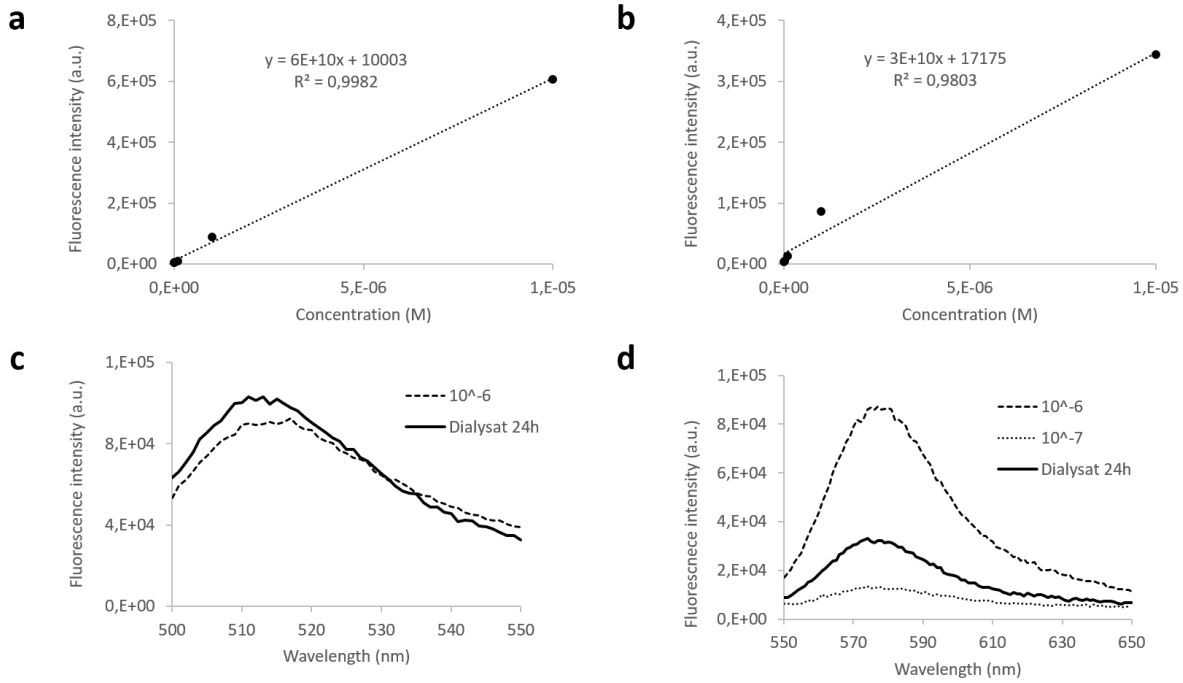

Figure S6: Estimation of the fraction of bound dye released from FITC-BSA/PDA NPs and RhBITC-BSA/PDA NPs after 4 months. (a), (b) The relationships between the fluorescence intensity and dye concentration were established for both FITC (a) and RhBITC (b) dyes. (c), (d) Dialysis was conducted with labelled NPs against 2 L of Milli-Q® water using a Spectra/Por® dialysis membrane with a molecular weight cut-off of 12–14 kDa. Based on the dye concentrations estimated to initially bind to NPs (164 µM of FITC and 373 µM of RhBITC), less than 1 % of dye (1.5 µM -0.9%- for FITC and 0.5 µM -0.1%- of RhBITC) was estimated to release from 4-months old labelled NPs.

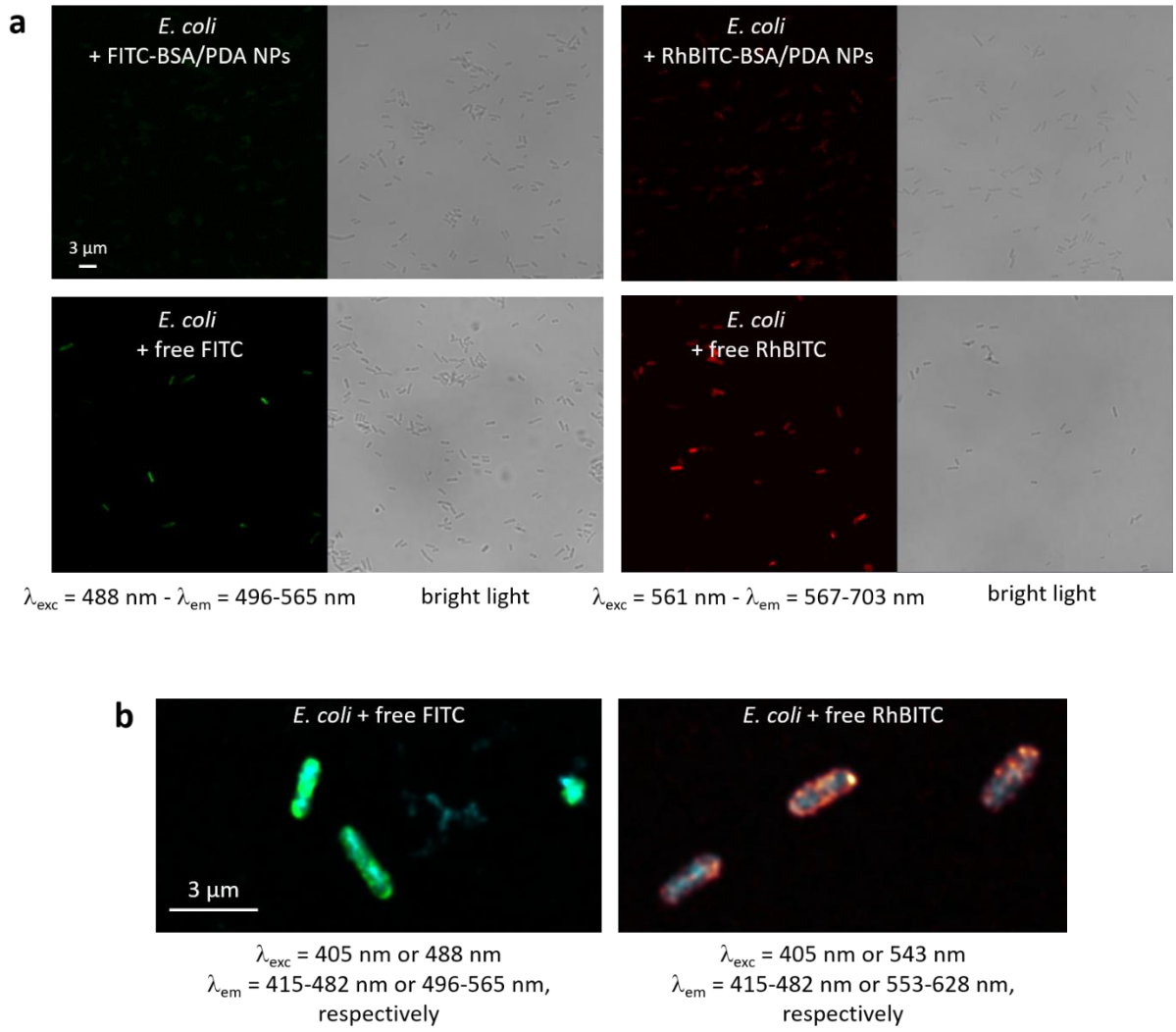

Figure S7: Micrographs of *E. coli* cells cultivated (a) with FITC-BSA/PDA NPs, RhBITC-BSA/PDA NPs, free FITC or free RhBITC and observed with standard CLSM (LSM710, Zeiss, Oberkochen, Germany), or (b) with free FITC or free RhBITC and observed with high-resolution CLSM (Stellaris 5, Leica Biosystems, Wetzlar, Germany).

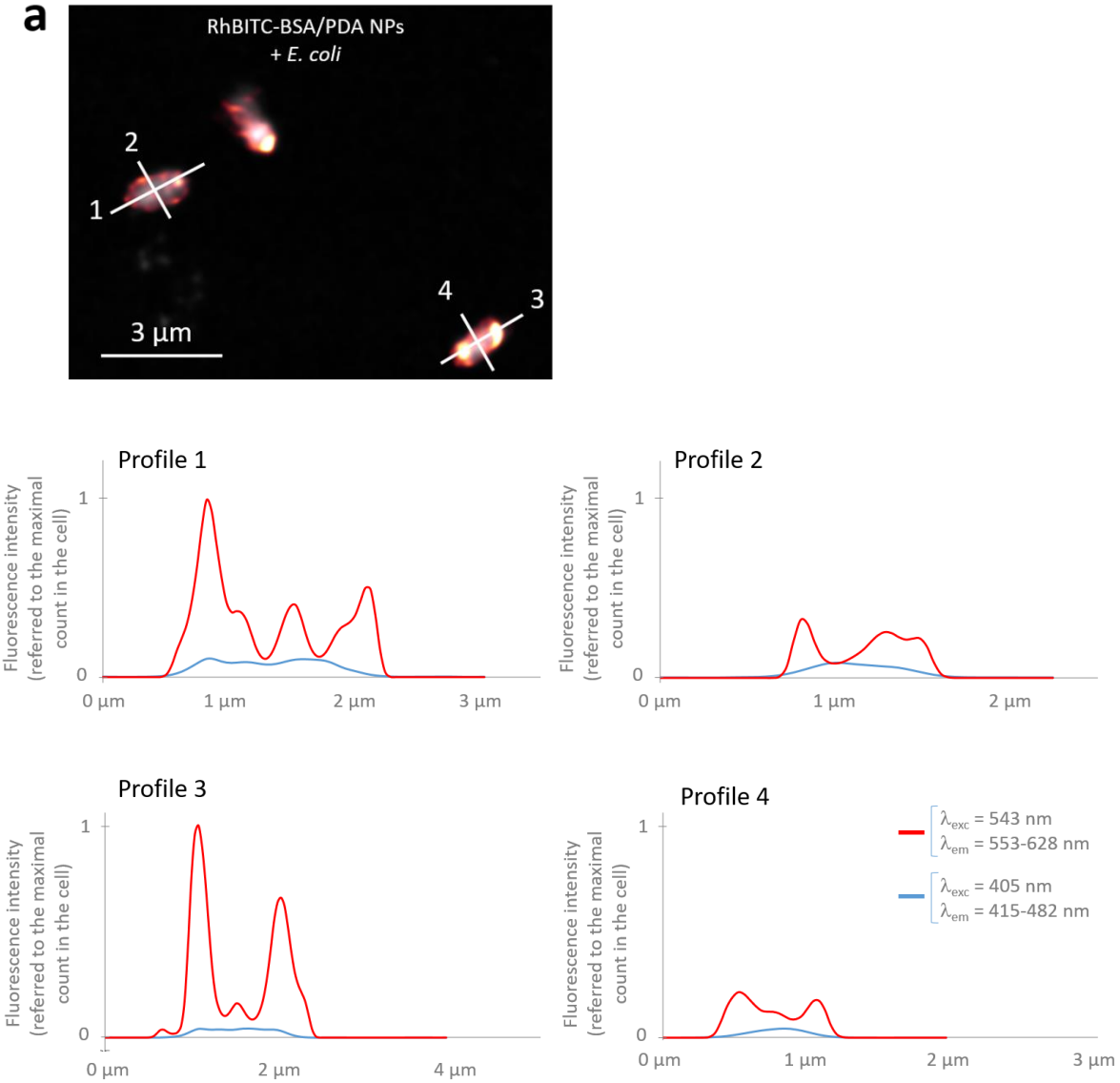
a
RhBITC-BSA/PDA NPs
+ E. coli
1
2
3
4
3 µm
Profile 1
Profile 2
Profile 3
Profile 4
Fluorescence intensity (referred to the maximal count in the cell)
0 µm
1 µm
2 µm
3 µm
4 µm
λexc = 543 nm
λem = 553-628 nm
λexc = 405 nm
λem = 415-482 nm

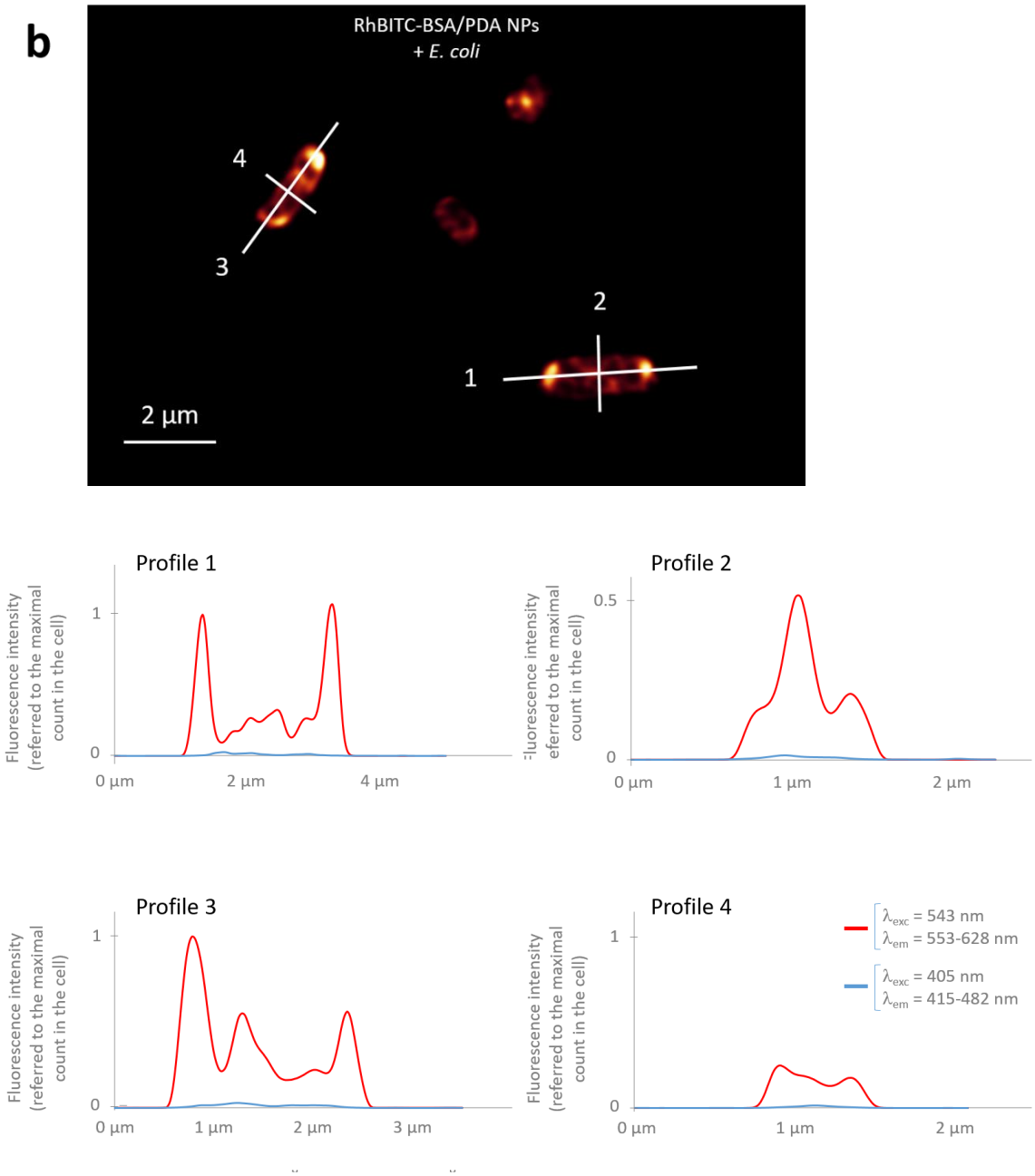
b
RhBITC-BSA/PDA NPs
+ E. coli
4
3
2
1
2 µm
Profile 1
Fluorescence intensity (referred to the maximal count in the cell)
1
0
0 µm
2 µm
4 µm
Profile 2
0.5
0
0 µm
1 µm
2 µm
Profile 3
0 µm
1 µm
2 µm
3 µm
Profile 4
λexc = 543 nm
λem = 553-628 nm
λexc = 405 nm
λem = 415-482 nm

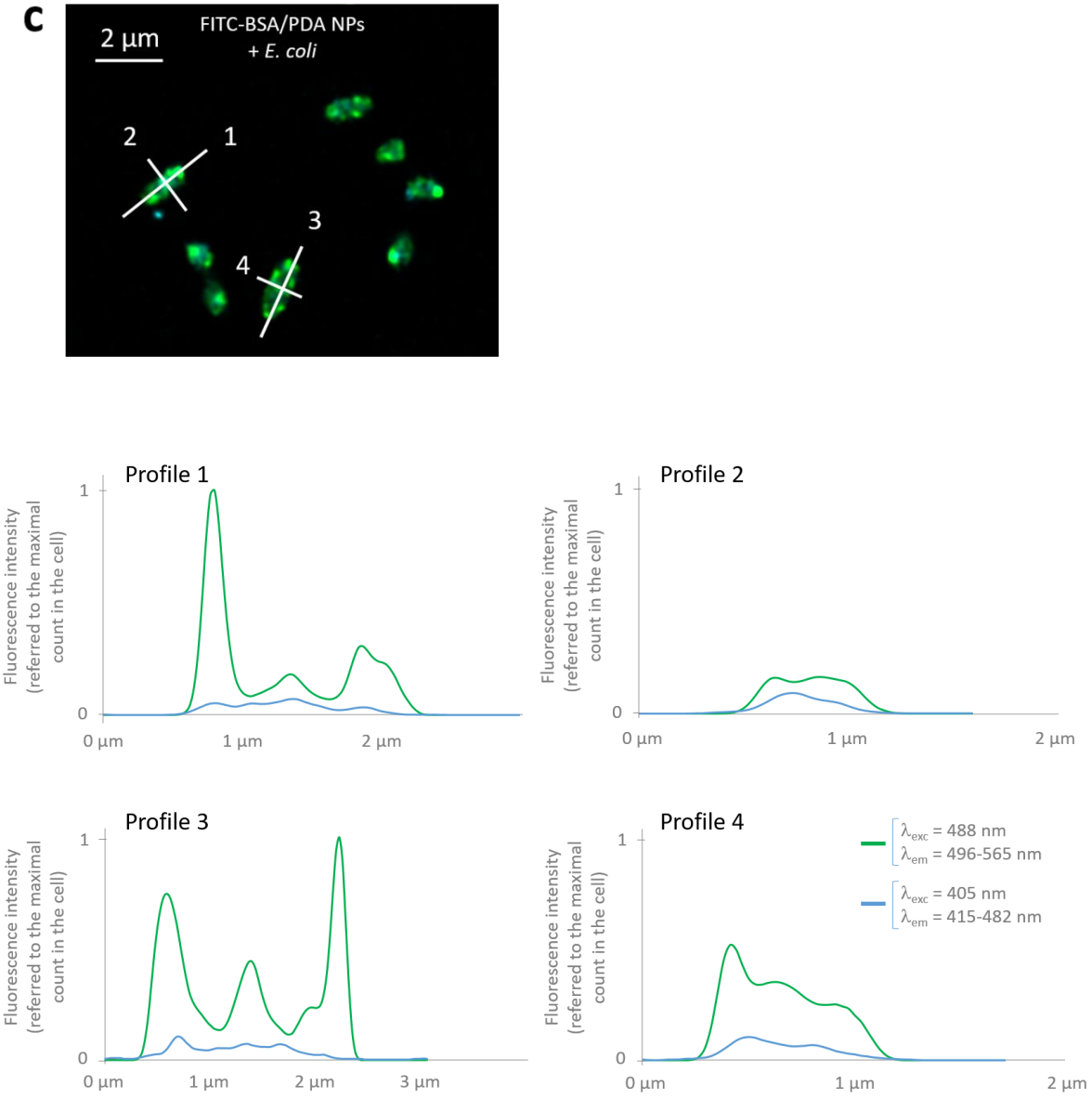
C
2 µm
FITC-BSA/PDA NPs
+ E. coli
1
2
3
4
Profile 1
Profile 2
Profile 3
Profile 4
Fluorescence intensity
(referred to the maximal
count in the cell)
1
0
0 µm
1 µm
2 µm
3 µm
λexc = 488 nm
λem = 496-565 nm
λexc = 405 nm
λem = 415-482 nm

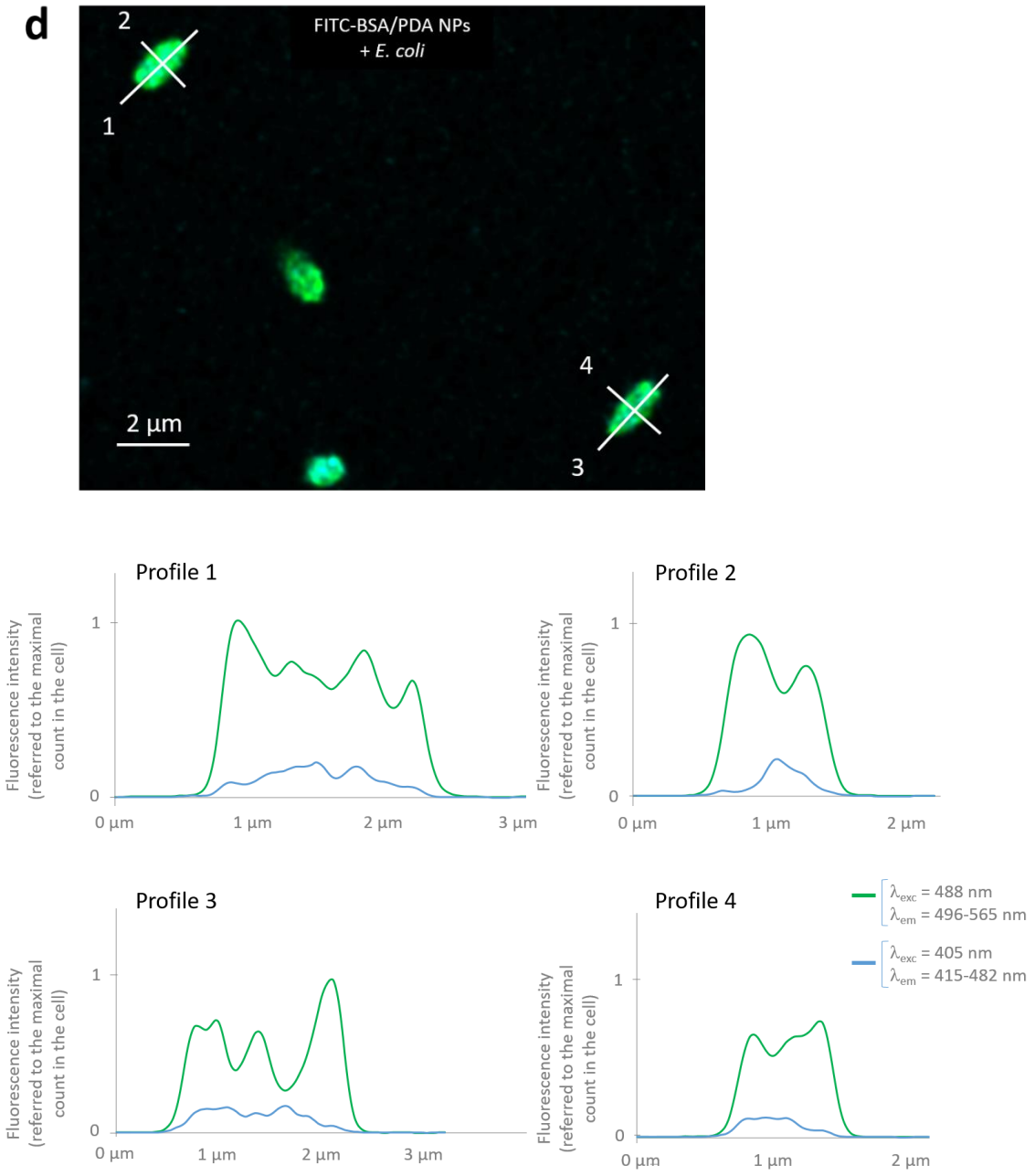

Figure S8: Typical profiles and patterns observed in micrographs of *E. coli* cells cultivated with RhBITC- or FITC-BSA/PDA NPs observed by high-resolution Stellaris 5 CLSM (Leica Biosystems, Wetzlar, Germany): (a) and (b) Two supplementary, typical examples of bacterials cells cultivated with RhBITC-BSA/PDA NPs (λ_{exc} = 405 nm and 543 nm; λ_{em} = 415–482 nm and 553–628 nm, respectively); (c) and (d) Two typical examples of bacterial cells cultivated with FITC-BSA/PDA NPs (λ_{exc} = 405 nm and 488 nm; λ_{em} = 415–482 nm and 496–565 nm, respectively).

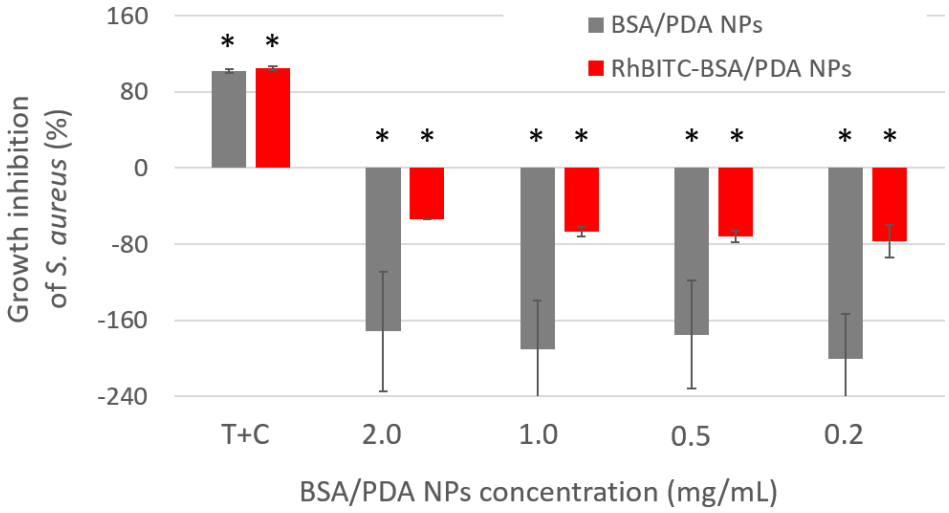

Figure S9: Growth inhibition of *S. aureus* populations with pristine BSA/PDA NPs and RhBITC-BSA/PDA NPs from 0.2 to 2 mg/mL concentration or with antibiotics (solution of 10 µg/mL tetracycline and 0.1 µg/mL cefotaxime) ("T+C"; positive control) compared to *S. aureus* culture without NPs. **: significant differences to *S. aureus* culture without NPs (p-value < 0.001).

References

1. Ma, B.; Liu, F.; Zhang, S.; Duan, J.; Kong, Y.; Li, Z.; Tang, D.; Wang, W.; Ge, S.; Tang, W.; Liu, H. *Journal of Materials Chemistry B* **2018**, *6* (40), 6459-6467. doi:10.1039/C8TB01930D